On Volatility induced Stationarity for Stochastic Differential Equations

Article · January 2007

CITATIONS
4

READS
41

4 authors, including:

Bjarne Jensen
Copenhagen Business School
29 PUBLICATIONS **127** CITATIONS
SEE PROFILE

Anders Muszta
Swedish University of Agricultural Sciences
11 PUBLICATIONS **142** CITATIONS
SEE PROFILE

Martin Richter
Copenhagen Business School
2 PUBLICATIONS **69** CITATIONS
SEE PROFILE

D-CAF Working Paper Series

On Volatility Induced Stationarity for Stochastic Differential Equations

J.M.P. Albin, B. Astrup Jensen, A. Muszta, and M. Richter

D-CAF Working Paper No. 10 June 2006

ON VOLATILITY INDUCED STATIONARITY FOR STOCHASTIC DIFFERENTIAL EQUATIONS

J.M.P. ALBIN,* *Chalmers University of Technology*

BJARNE ASTRUP JENSEN,** *Copenhagen Business School*

ANDERS MUSZTA,*** *Chalmers University of Technology*

MARTIN RICHTER,**** *Copenhagen Business School*

Abstract

This article deals with stochastic differential equations with volatility induced stationarity. We study of theoretical properties of such equations, as well as numerical aspects, together with a detailed study of three examples.

Keywords: CIR model; CKLS model; heavy-tailed SDE; hyperbolic SDE; local martingale; mean reversion; numerical methods; stochastic differential equation; time changed SDE; volatility induced stationarity

2000 Mathematics Subject Classification: Primary 60G44; 60H10; 60H35; 60J60; 65C30; 68U20. Secondary 60J65; 62P05; 65C40

1. Introduction

This article deals with stochastic differential equations (SDE) with volatility induced stationarity (*vis*). Although the *vis* effect is more or less well-known, misinterpretations

* Postal address: Mathematical Sciences, Chalmers University of Technology, 412 96 Gothenburg, Sweden. Email and www: palbin@math.chalmers.se and http://www.math.chalmers.se/~palbin

** Postal address: Department of Finance, Copenhagen Business School, 2000 Frederiksberg, Denmark. Email: ba.fi@cbs.dk

*** Postal address: Mathematical Sciences, Chalmers University of Technology, 412 96 Gothenburg, Sweden. Email: muszta@math.chalmers.se

**** Postal address: Department of Finance, Copenhagen Business School, 2000 Frederiksberg, Denmark. Email: mr.fi@cbs.dk

in the literature are common. We clerify matters by giving a general definition of *vis*, and explain why SDE with *vis* have a local martingale term that is not a martingale. We investigate the relation between *vis* and stationary moments and mean reversion.

SDE with *vis* feature to model, for example, interest rates and eletricity prices. But, such SDE can be difficult from a statistical point of view, so that basic estimation procedures fail. Hence computer simulations to evaluate statistics are important. As standard simulation schemes can fail for SDE with *vis*, we discuss alternative schemes.

We provide three examples of SDE with *vis*, that all are different in terms of their *vis* effect, and that require different simulation procedures. The main example is the CKLS model, which has been studied by many authors, but where we find some new features. The others are a class of hyperbolic SDE, and a class of heavy-tailed SDE.

This article is organized as follows: After the preliminary Section 2, we define *vis* in Section 3, and adress connections to boundaries for the diffusion and existence of moments. Section 4 deals with theoretical aspects of computer simulation of SDE with *vis*, together with properties of the local martingale term and mean reversion. In Section 5-7 we study the three examples that have been mentioned, of SDE with *vis*.

2. Preliminaries

In this section we set some notation that is required in later sections.

Let $\{W_t\}_{t\geq 0}$ be standard Brownian motion and $I=(l,r)$, $-\infty \leq l < r \leq \infty$ an open interval. For measurable functions $b: I \to \mathbb{R}$ and $\sigma : I \to [0,\infty)$, consider the SDE

$$dX_t = b(X_t)\,dt + \sigma(X_t)\,dW_t, \quad X_0 = \zeta, \tag{2.1}$$

where ζ is a random variable with values in I that is independent of W. The law of X is denoted $\mathbf{P}^\zeta$, while the probability distribution of X_t is denoted $P_t(\zeta,\cdot)$. Further, π denotes the stationary distribution for X, when it exists.

A property holds *locally on* I if the property is true on all compact subsets of I.

Assumption 2.1. *The* drift b *is continuous and the* volatility σ *is (strictly) positive and locally Hölder continuous of order* $\frac{1}{2}$.

Given an $x_0 \in I$, the *scale* function S and *speed* measure m are given by

$$S(x) = \int_{x_0}^{x} \exp\left\{-2\int_{x_0}^{y} \frac{b(z)}{\sigma(z)^2}\,dz\right\} dy \quad \text{and} \quad \frac{dm(x)}{dx} = \frac{2}{\sigma(x)^2 S'(x)} \quad \text{for } x \in I.$$

Feller's test for non-explosion requires the following function v to go to infinity

$$v(x) = \int_{x_0}^{x} S'(y)\left(\int_{x_0}^{y} dm(z)\right) dy = \int_{x_0}^{x} (S(x) - S(y))\, dm(y) \quad \text{for } x \in I\text{:}$$

Assumption 2.2. *We have* $v(l^+) = \lim_{x \downarrow l} v(x) = \infty$ *and* $v(r^-) = \lim_{x \uparrow r} v(x) = \infty$.

Assumptions 2.1 and 2.2 are sufficient for the existence of a unique strong solution of (2.1) that does not explode (see e.g., Karatzas and Shreve, 1991, Section 5.5).

Assumption 2.3. *We have* $S(l^+) = -\infty$, $S(r^-) = \infty$ *and* $m(I) < \infty$.

If we strengthen Assumption 2.2 to Assumption 2.3, the stationary solution to (2.1), with $\zeta \stackrel{\mathrm{d}}{=} \pi = m/m(I)$, is *ergodic* (see e.g., Rogers and Williams, 1987, p. 300), i.e.,

$$\lim_{t \to \infty} \frac{1}{t} \int_0^t f(X_s)\, ds = \int_I f(x)\, dm(x) \quad \text{for measurable } f : I \to \mathbb{R},$$

and β-*mixing*, so that the β-mixing coefficient

$$\beta(t) = \int_I \| dP_t^x(y) - d\pi(y) \|_{\mathrm{TV}}\, d\pi(x)$$

satisfies $\lim_{t \to \infty} \beta(t) = 0$, where $\| \cdot \|_{\mathrm{TV}}$ is the total variation norm (see e.g., Doukhan, 1994, Sections 2.4 and 2.5, and Rogers and Williams, 1987, p. 303).

The *infinitesimal generator* $\mathcal{L}f = bf' + \frac{1}{2}\sigma^2 f''$ has a *spectral gap* if it has a strictly negative second largest (to 0) eigenvalue λ. This is so if and only if the solution to (2.1) is ρ-*mixing*, that is, the ρ-mixing coefficient

$$\rho(t) = \sup\left\{ \frac{\| P_t f \|_{\mathbb{L}^2(I,\pi)}}{\| f \|_{\mathbb{L}^2(I,\pi)}} : f \in \mathbb{L}^2(I,\pi), \langle f, 1 \rangle_{\mathbb{L}^2(I,\pi)} = 1 \right\}$$

satisfies $\lim_{t \to \infty} \rho(t) = 0$, where $P_t f(x) = \int_I f(y)\, dP_t^x(y)$, as $\rho(t) = \mathrm{e}^{\lambda t}$, see Genon-Catalot, Jeantheau and Larédo (2000), Section 2.4. See Hansen, Scheinkman and Touzi (1998) and Genon-Catalot, Jeantheau and Larédo on more on spectral gaps.

3. Volatility induced stationarity

In this section we generalize the definition of *vis*, given by Conley, Hansen, Luttmer and Scheinkman (1997) for the special case of the CKLS model [see (5.1) below]. Throughout this section, we assume that Assumptions 2.1 and 2.3 hold.

Usually when describing the dynamics of an SDE, we split it into an ordinary differential equation (ODE) for the drift, and a diffusion white noise perturbation of the ODE.

We expect the ODE to have a non-exploding solution that converges to the stationary mean of the SDE. This interpretation corresponds to an Euler approximation of the SDE. But when adding more terms to the Itô-Taylor expansion of the SDE (see Kloeden and Platen, 1995, Section 5.5), the picture changes, as this shows that the drift part and diffusion part interact.

The simplified interpretation of the SDE is often fruitful, but is some times incorrect. This lead Conley, Hansen, Luttmer and Scheinkman (1997) to define the concept of *vis* for the CKLS model. Building on their ideas, we make a general definition of *vis*:

Definition 3.1. The stationary solution to the SDE (2.1) has *vis* at l $[r]$, and we call l $[r]$ a *vis boundary*, if $S'(l^+) < \infty$ $[S'(r^-) < \infty]$. If $S'(l^+) > 0$ $[S'(r^-) > 0]$ we call l $[r]$ a *positive vis boundary* − otherwise it is a *null vis boundary*.

One may make a more general definition using lim inf and lim sup instead of limits. Because of Assumption 2.3, we can only have *vis* boundaries at $\pm\infty$. In addition, since $m(I) < \infty$, to have *vis* at l $[r]$ it is necessary that $\sigma(l+) = \infty$ $[\sigma(r_-) = \infty]$.

For *vis* the mean reversion associated with stationarity comes from high volatility rather than from the drift. SDE with *vis* do not behave as white noise perturbed ODE.

Example 3.1. A local martingale in natural scale (i.e., zero drift) has *positive vis boundaries* at $\pm\infty$. A local martingale in natural scale with other boundaries than $\pm\infty$ cannot be stationary: An example of the latter is $dX_t = |X_t|dW_t$ with $X_t = 1$, for which $m(I) = m((0,\infty)) = \infty$.

For a diffusion in natural scale with *vis*, large values of the process give a high volatility and a small speed measure. Hence the diffusion moves away quickly from this area, in a direction that is locally unbiased, so that the process is a local martingale. But if the process moves towards an even higher value, then the volatility gets even larger and the speed measure even smaller, so that the time spent at large values is short: If the volatility gets large fast enough, it is possible to achieve stationarity. Still, the process can take very large values, during very short period of time. In addition, the fact that the process has a very high volatility for large values of the process, in the described fashion, makes it likely that, within short, the process takes on a smaller value. This will prevent the local martingale from being a martingale!

Proposition 3.1. *Under Assumptions 2.1 and 2.3, if X is the solution to (2.1) with fixed initial value $\zeta = x$, then the local martingale $Y = S(X)$ is a martingale if and only if l and r are natural boundaries for X.*

Proof. We have entrance [natural] boundary for X at l and $[r]$, if and only if the local

martingale $Y = S(X)$, with natural scale $S_Y(y) = y$ and speed measure $dm_Y(y) = 2/(\sigma(y)S'(y))dy$, has entrance [natural] boundary at $-\infty$ [∞], if and only if

$$\infty > \ [\infty =] \ \int_{-\infty}^{0} |x| \, dm_Y(x) \ \left[\int_0^{\infty} x \, dm_Y(x) \right]$$

(see e.g., Karlin and Taylor 1981). By Arbib (1965), Theorem 3, X is a martingale if l and r are natural boundaries for X, so that $\pm\infty$ are natural boundaries for Y. Conversely, assume that e.g., ∞ is not a natural boundary for Y, so that $\int_0^{\infty} x \, dm_Y(x) < \infty$. Using Revuz and Yor (1999), p. 429, Exercise 3.18, considering the additive functionals $A_t = \int_0^t Y_s^+ \, ds$ and $C_t = t$ of Y, we then have

$$\lim_{t\to\infty} \mathbf{E}^y\{A_t\}/\mathbf{E}^y\{C_t\} = \lim_{t\to\infty} \frac{1}{t} \int_0^t \mathbf{E}^y\{Y_s^+\} \, ds = \int_0^{\infty} x \, dm_Y(x) \quad \text{for } \ y \in \mathbb{R}. \tag{3.1}$$

If Y is a martingale, then Y^+ is a submartingale, so that $\mathbf{E}^y\{Y_s^+\}$ is non-decreasing, and $\mathbf{E}^y\{Y_s^+\} \geq y$. But this contradicts (3.1) if we select $y > \int_0^{\infty} x \, dm_Y(x)$. □

We have the following interesting easy consequence of Proposition 3.1 and (3.1):

Corollary 3.1. *Under Assumptions 2.1 and 2.3, if X is the stationary solution to (2.1) and l and r are natural boundaries, then the stationary local martingale $Y = S(X)$ has infinite mean and is thus not a matingale.*

We have the following useful result:

Proposition 3.2. *Under Assumptions 2.1 and 2.3, a positive vis boundary l [r] is an entrance [a natural] boundary if and only if*

$$\infty > \ [\infty =] \quad \int_l^{x_0} \frac{-x}{\sigma(x)^2} \, dx \quad \left[\int_{x_0}^{r} \frac{x}{\sigma(x)^2} \, dx \right]. \tag{3.2}$$

A null vis boundary l [r] is natural if the integral [integral] in (3.2) is infinite.

Proof. By definition, l [r] is an entrance [a natural] boundary if

$$\infty > \ [\infty =] \quad \int_l^{x_0} \frac{S(x_0) - S(x)}{\sigma(x)^2 S'(x)} \, dx \quad \left[\int_{x_0}^{r} \frac{S(x) - S(x_0)}{\sigma(x)^2 S'(x)} \, dx \right]. \tag{3.3}$$

If l [r] is a positive vis boundary, then the criteria (3.2) follows from the fact that

$$\frac{-S(l^+)x}{2\sigma(x)^2} \leq \frac{S(x_0)-S(x)}{\sigma(x)^2 S'(x)} \leq \frac{-2S(l^+)x}{\sigma(x)^2} \qquad \left[\frac{S(r^+)x}{2\sigma(x)^2} \leq \frac{S(x)-S(x_0)}{\sigma(x)^2 S'(x)} \leq \frac{2S(r^+)x}{\sigma(x)^2}\right]$$

for $x > l$ small enough [$x < r$ large enough]. If l [r] is a null vis boundary, then we get

$$\frac{S(x_0)-S(x)}{\sigma(x)^2 S'(x)} \geq \frac{-S(l^+)x}{\sigma(x)^2} \qquad \left[\frac{S(x)-S(x_0)}{\sigma(x)^2 S'(x)} \geq \frac{S(r^+)x}{\sigma(x)^2}\right]$$

for $x > l$ small enough [$x < r$ large enough], so that the integral [integral] in (3.3) is infinite if the integral [integral] in (3.2) is infinite. □

Example 3.2. Given a constant $p>1$, Assumptions 2.1 and 2.3 hold for the SDE

$$dX_t = (1 + |X_t|^p)\, dW_t, \quad X_0 = \zeta, \tag{3.4}$$

and $\pm\infty$ are positive *vis* boundaries (cf. Example 3.1). By Proposition 3.2, $\pm\infty$ are natural boundaries for $1 < p \leq 2$, and entrance boundaries for $p > 2$. Hence, solutions to (3.4) with fixed initial values $\zeta = x$ are martingales for $1 < p \leq 2$, and local martingales that are not martingales for $p > 2$, by Proposition 3.1.

A stationary local martingale with finite variance is either constant or not a martingale, see Bibby and Sørensen (1997), Lemma 2.1. Thus the stationary solution X is never a martingale. But it is uniformly integrable, by stationarity.

By Hansen, Scheinkman and Touzi (1998), Sections 4.1-4.2 and Example 4, we have a spectral gap and ρ-mixing for $p \geq 2$, but no spectral gap for $p < 2$.

For diffusions with drift the interpretation of *vis* is the same as for local martingales, as by the definition of *vis*, the volatility will dominate the drift close to *vis* boundaries.

If there is *vis* only at one boundary point, then the local martingale term of the solution to the SDE (2.1) will be biased, giving the solution a local martingale term with a decreasing or increasing mean, taking it away from the *vis* boundary.

There can be statistical problem for SDE with *vis*. For example, functions in the domain of the generator are important for statistical inference. But for SDE with *vis*, the only polynomials in the domain are constants, as functions f in the domain satisfy $(f'/S')(r^-) = (f'/S')(l^+) = 0$, see Hansen, Scheinkman and Touzi (1998), p. 10.

4. Simulation of SDE with *vis*

In this section we discuss computer simulation of SDE with *vis*. Such simulations can be difficult because standard requirements for convergence, such as Lipschitz conditions and linear growth for the drift and volatility, are not satisfied.

Let $\Delta W_n = W_{t_{n+1}} - W_{t_n}$ for equidistant times $0 = t_0 < t_1 < \ldots < t_N = T$ with spacing $\Delta > 0$. For $\theta_b, \theta_\sigma \in [0,1]$, a family of Euler schemes, starting at Y_0, are given by

$$Y_{n+1} = Y_n + \big(\theta_b \bar{b}(Y_{n+1}) + (1-\theta_b)\bar{b}(Y_n)\big)\,\Delta + (\theta_\sigma \sigma(Y_{n+1}) + (1-\theta_\sigma)\sigma(Y_n))\,\Delta W_n \quad (4.1)$$

for $n < N$: Here $\bar{b} = b - \theta_\sigma \sigma\sigma'$ is a correction term to ensure convergence to an Itô integral. For $\theta_b = \theta_\sigma = 0$ we get the *Euler* scheme, for $\theta_\sigma = 0$ the stochastic *theta* method, see Higham (2000), and for $\theta_b = \theta_\sigma = 1$ the *fully implicit Euler* scheme.

The *backward Euler* scheme (BE) is the theta method with $\theta_b = 1$. The *split step backward Euler* scheme (SSBE), studied by Mattingly, Stuart and Higham (2002), is given by

$$Y_{n+1} = Y_n + \sigma(Y_n^*)\Delta W_n \quad \text{where} \quad Y_n^* = Y_n + b(Y_n^*)\Delta \quad \text{for } n < N.$$

For $I \subsetneq \mathbb{R}$ we prefer the fully implicit Euler scheme to the SSBE scheme, as the latter can move out of I. But the implicit Euler scheme has the drawback that the implicit equation may not have a unique solution: We discuss this issue in Section 5.

Higham, Mao and Stuart (2002), Theorem 2.2, prove uniform strong convergence of the Euler scheme, for locally Lipschitz drift and volatility, when the suprema of the true solution and the Euler scheme, started at a fixed $\zeta = x$, have moments of some order $p > 2$. With the additional assumptions that the drift is one-sided Lipschitz,

$$(x-y)(b(x)-b(y)) \le C\,|x-y|^2 \quad \text{for } x, y \in I, \text{ for some constant } C > 0,$$

and the volatility is globally Lipschitz, Higham, Mao and Stuart (2002) further show existence of all moments of the solution and of the SSBE approximation. Finally they examine convergence of implicit Euler schemes, which we will return to later.

Gyöngy (1998) shows uniform almost sure convergence of the Euler scheme assuming that the (continuous) drift is one-sided Lipschitz and the volatility locally Lipschitz.

An important issue, besides convergence of the numerical scheme, is to have an approximation with the same boundary properties as the true solution. Normally the Euler scheme will induce a recurrent Markov chain on $\mathbb{R}$.

However, for many SDE the probability to end up outside I is negligible already for moderately small Δ. Stability of simulation schemes has been studied by Higham

(2000), Mattingly, Stuart and Higham (2002) and Talay (2002). The next results show that, for many diffusions with *vis* boundaries at infinity, the Euler scheme can be transient.

Proposition 4.1. *Let $\{Y_n\}_{n\geq 0}$ be the Euler approximation of the SDE with (2.1) with σ strictly poitive. If there exist constants $p > 0$ and $\phi > 0$ such that*

$$\lim_{x\to\pm\infty} \frac{|x|^p\,|b(x)|}{|\sigma(x)|} = 0 \quad \textit{and} \quad \liminf_{x\to\pm\infty} \frac{|b(x)|}{|x|} \geq \phi, \tag{4.2}$$

then

$$\mathbf{P}\Big\{\bigcap_{n\geq 0}\{|Y_{n+1}| \geq (1+\tilde{\phi})|Y_n|\}\Big\} > 0 \quad \textit{for } \tilde{\phi} \in (0,\phi).$$

Proof. Given constants $c > 0$ and $y_0 > 0$, let

$$a_n = c \sup_{|x|\geq(1+\phi)^n y_0} \frac{|b(x)|}{|\sigma(x)|} \quad \text{for } n \geq 0. \tag{4.3}$$

By (4.2) there exist constants $c_1 > 0$ and $k > 0$ such that

$$\sup_{|x|\geq c_1} \frac{|x|^p\,|b(x)|}{|\sigma(x)|} < k.$$

Taking $y_0 \geq c_1$, this gives

$$\sum_{n=0}^{\infty} a_n = \sum_{n=0}^{\infty} \sup_{|x|\geq(1+\phi)^n y_0} \frac{|x|^p\,|b(x)|}{|\sigma(x)|}\,|x|^{-p} \leq \sum_{n=0}^{\infty} \sup_{|x|\geq(1+\phi)^n y_0} k\,|x|^{-p} = k\sum_{n=0}^{\infty}(1+\phi)^{-np} y_0$$

is finite. From this it is an elementary exercise to see that

$$\mathbf{P}\Big\{\bigcap_{n\geq 0}\{|\Delta W_n| \geq a_n\}\Big\} > 0. \tag{4.4}$$

And so it is enough to show that

$$|Y_{n+1}| \geq (1+\tilde{\phi})\,|Y_n| \quad \text{on} \quad \bigcap_{n\geq 0}\{|\Delta W_n| \geq a_n\}. \tag{4.5}$$

We now specify the choice of c and y_0 in (4.3): Pick $\tilde{\phi} \in (0,\phi)$ and put $c = 1+\Delta+2/\tilde{\phi}$. As $\sigma > 0$, the Euler scheme will hit any interval with positive probability. Therefore, we can without loss assume that the Euler scheme start at some $Y_0 = y_0$. Now choose $y_0 \geq c_1$ such that $|b(x)|\,/\,|x| \geq \tilde{\phi}$ for $|x| \geq y_0$ [cf. (4.2)].

First assume that $Y_{n+1}/Y_n \geq 1$, so that (4.5) reduces to $Y_{n+1}/Y_n - 1 \geq \tilde{\phi}$. Since

$$|\Delta W_n| \geq a_n \geq (1 + \Delta + \frac{2}{\tilde{\phi}})\frac{|b(Y_n)|}{|\sigma(Y_n)|},$$

(4.5) follows from the following calculation:

$$\frac{Y_{n+1}}{Y_n} - 1 = \frac{|\sigma(Y_n)|}{|Y_n|}\left|\frac{b(Y_n)}{\sigma(Y_n)}\Delta + \Delta W_n\right| \geq \frac{|\sigma(Y_n)|}{|Y_n|}\frac{|b(Y_n)|}{|\sigma(Y_n)|} \geq 2 + \tilde{\phi} \geq \tilde{\phi}.$$

For $Y_{n+1}/Y_n < 1$ we have

$$\begin{aligned}&\left|\frac{Y_{n+1}}{Y_n} - 1\right| \\ &= \left|\frac{b(Y_n)}{Y_n}\Delta + \frac{\sigma(Y_n)}{Y_n}\Delta W_n\right| \geq \left|\frac{\sigma(Y_n)}{Y_n}\right|\left(1 + \frac{2}{\tilde{\phi}}\right)\left|\frac{b(Y_n)}{\sigma(Y_n)}\right| = \left|\frac{b(Y_n)}{Y_n}\right|\left(1 + \frac{2}{\tilde{\phi}}\right) \geq 2 + \tilde{\phi},\end{aligned}$$

so that $Y_{n+1}/Y_n < -1$, since $Y_{n+1}/Y_n < 1$. From this in turn, we get (4.5) again:

$$\frac{|Y_{n+1}|}{|Y_n|} - 1 = \left|2 + \frac{b(Y_n)}{Y_n}\Delta + \frac{\sigma(Y_n)}{Y_n}\Delta W_n\right| \geq \tilde{\phi}. \quad \square$$

Many processes with *vis* are stationary local martingales. The following result shows that for these processes the Euler scheme can usually be transient.

Proposition 4.2. *Let $\{Y_n\}_{n\geq 0}$ be the Euler approximation of the SDE (2.1) with zero drift $b = 0$ and $\sigma > 0$. If*

$$\lim_{x\to\pm\infty} |x|^p / \sigma(x) = 0 \quad \textit{for some } p > 1, \tag{4.6}$$

then

$$\mathbf{P}\left\{\bigcap_{n\geq 0}\{|Y_{n+1}| \geq (1+\phi)Y_n\}\right\} > 0 \quad \textit{for } \phi > 0.$$

Proof. Pick a $\phi > 0$. As in the proof of Proposition 4.1 we may assume that the Euler scheme starts at some suitable $y_0 > 0$. Define

$$a_n = (2 + \phi) \sup_{|x|\geq(1+\phi)^n y_0} \frac{|x|}{\sigma(x)} \quad \text{for } n \geq 0.$$

From (4.6) it follows that $\sum_{n\geq 0} a_n < \infty$, so that (4.4) holds. And so the proposition follows from the methodology used for the proof of Proposition 4.1. $\square$

For the SDE in Propositions 4.1 and 4.2, instability starts when the Euler scheme is numerical large, making it oscillate between large positive and negative values.

For stationary diffusions in natural scale that are not too heavy tailed, the Euler scheme can be transient, as we have the following easy corollary to Proposition 4.2:

Corollary 4.1. *The Euler scheme is transient with positive probability, for a local martingale X given by (2.1), that admits a stationary distribution π such that*

$$\int_{-\infty}^{\infty} |x|^p \, d\pi(x) < \infty \quad \textit{for some } \; p > 1.$$

By the results of Gyöngy (1998), the Euler scheme converges almost surely as $\Delta \downarrow 0$. But for many SDE with *vis*, for any specific Δ, the Euler scheme may diverge.

Some times one can make a bijective transformation of X to another process with constant volatility and a drift that is one-sided Lipschitz: If Assumption 2.1 holds and the volatility in (2.1) has an absolutely continuous derivative, then the function $f(z) = \int^z 1/\sigma(x)\, dx$ is strictly increasing and $Z_t = f(X_t)$ satisfies the SDE

$$dZ_t = \left(\frac{b(f^{-1}(Z_t))}{\sigma(f^{-1}(Z_t))} - \frac{1}{2}\sigma'(f^{-1}(Z_t)) \right) dt + dW_t, \qquad Z_0 = f(\zeta). \tag{4.7}$$

If the drift in (4.7) is one-sided Lipschitz, then the BE and SSBE schemes will usually work well, see Mattingly, Stuart and Higham (2002).

5. The CKLS model

In Sections 5-7 we study three examples of SDE with various degrees of *vis*, and different sample path properties with different simulation and modelling problems.

For simulations we use the pseudo random number generator *ran2* from Flannery, Press, Teukolsky and Vetterling (1995). All simulations use the same underlying Brownian motion, so that they are started with the same seed $d = -1$. Even though we supply just a few figures, our numerical experience build on many more simulations.

Extending the *CIR* model of Feller (1951) and Cox, Ingersoll and Ross (1985), given constants $\alpha, \beta \in \mathbb{R}$ and $\sigma, \gamma > 0$, Chan, Koralyi, Longstaff and Sanders (1992) studied the *CKLS* model

$$dX_t = (\alpha + \beta X_t)\, dt + \sigma X_t^{\gamma}\, dW_t, \quad X_0 = \zeta > 0. \tag{5.1}$$

We first find boundaries, moments and the stationary distribution of the process. Then we study simulation problems. The CKLS model has a medium degree of *vis*.

5.1. Boundaries, ergodicity, moments and stationarity

We will consider the parameter values for which the SDE (5.1) has *vis*, which are

$$\{\tfrac{1}{2}<\gamma<1, \alpha>0, \beta=0\}\cup\{\gamma=1, \alpha>0, 0\le\beta<\tfrac{1}{2}\sigma^2\}\cup\{\gamma>1, \alpha>0\}\cup\{\gamma>1, \alpha=0, \beta>0\}.$$

For these parameters, Assumptions 2.1 and 2.3 hold, and we have ρ-mixing, see Hansen, Scheinkman and Touzi (1998). The boundary 0 is an entrance boundary for $\alpha > 0$ and natural for $\alpha = 0$. The *vis* boundary ∞ is null for $\gamma = 1$ and positive otherwise. By Proposition 3.2, ∞ is an entrance boundary for $\gamma > 1$ and natural for $\gamma \le 1$.

One way to explain the *vis* for the CKLS model is to consider the transformed process $Z_t = f(X_t)$, where $f(x) = x^{1-\gamma}$ $\gamma \ge \frac{1}{2}$, $\gamma \ne 1$. By Itô's lemma we have

$$dZ_t = \varphi(Z_t)\,dt + (1-\gamma)\sigma\,dW_t, \tag{5.2}$$

where

$$\varphi(z) = \alpha(1-\gamma)z^{\gamma/(\gamma-1)} + (1-\gamma)\beta z + \frac{1}{2}\gamma(\gamma-1)\sigma^2 z^{-1}. \tag{5.3}$$

Except for a constant, this is the transformation in (4.7). For $\gamma > 1$, close to zero, the term z^{-1} in the drift pushes the process away from zero. For large values, the process is pushed down towards zero, by the term $z^{\gamma/(\gamma-1)}$ for $\alpha > 0$, and by the term z for $\alpha = 0$. For $\frac{1}{2} < \gamma < 1$, close to zero, the term $z^{\gamma/(\gamma-1)}$ pushes the process away from zero, but there is no strong downforce from high levels.

We find a formula for moments of the CKLS model below, as well as the stationary distribution, which can be used to check the fit of the CKLS model to data.

The stationary mean is infinite for $\gamma \le 1$: Moments of order $p < 2\gamma - 1$ exist for $\{\frac{1}{2} < \gamma < 1, \alpha > 0, \beta = 0\}$, and of order $p < 1 - 2\beta/\sigma^2$ for $\{\gamma = 1, \alpha > 0, 0 \le \beta < \frac{1}{2}\sigma^2\}$.

Proposition 5.1. *The local martingale part of the stationary solution is not a martingale.*

Proof. For $\gamma > 1$, we get this from that $\int_0^t X_s^\gamma\,dW_s$ has a decreasing mean over time, by Corollary 5.1 below. For $\gamma \le 1$, if $\sigma\int_0^t X_s^\gamma\,dW_s$ were a martingale, we would have

$$\mathbf{E}^\pi\left\{X_t - X_0 - \int_0^t \beta X_s\,ds\right\} = \alpha t + \mathbf{E}^\pi\left\{\int_0^t \sigma X_s^\gamma\,dW_s\right\} = \alpha t. \tag{5.4}$$

For $\beta = 0$, this contradicts stationarity, exactly as in Section 6.2 below. For $\beta \ne 0$, (5.4) with $t = 1$ and Fubini's theorem give $\mathbf{E}^\pi\{X_1 - X_0 - \beta X_{t_0}\} < \infty$ for almost all $t_0 \in (0,1)$. Subtracting this from (5.4), and using Fubini's theorem again, we get $\mathbf{E}^\pi\{X_s - X_{t_0}\} < \infty$ for almost all $s \in (0,1)$. If some mean $\mathbf{E}^\pi\{X_s - X_{t_0}\} \ne 0$ we

would get a linear behavior like (7.3), by recursion, which we reject, as in Section 6.2. And so, for almost all $s \in (0,1)$,

$$\alpha s = \mathbf{E}^\pi\Big\{ X_s - X_{t_0} - \int_0^s \beta(X_r - X_{t_0})\,dr + (1-\beta s)X_{t_0} - X_0 \Big\} = \mathbf{E}^\pi\{(1-\beta s)X_{t_0} - X_0\}.$$

But considering two distinct values of s, we get the contradiction $\mathbf{E}^\pi\{X_{t_0}\} < \infty$. □

Writing $\Gamma(\cdot)$ [$\Gamma(\cdot,\cdot)$] for the gamma function [incomplete gamma function], denote

$$M(p) = \sum_{k=0}^\infty \frac{1}{k!}\bigg[\frac{-\beta}{\sigma^2(\gamma-1)}\bigg(\frac{\sigma^2(2\gamma-1)}{2\alpha}\bigg)^{(2\gamma-2)/(2\gamma-1)}\bigg]^k \Gamma\bigg(k\frac{2\gamma-2}{2\gamma-1}+1-\frac{p}{2\gamma-1}\bigg),$$

$$M(p,x) = \sum_{k=0}^\infty \frac{1}{k!}\bigg[\frac{-\beta}{\sigma^2(\gamma-1)}\bigg(\frac{\sigma^2(2\gamma-1)}{2\alpha}\bigg)^{(2\gamma-2)/(2\gamma-1)}\bigg]^k \Gamma\bigg(k\frac{2\gamma-2}{2\gamma-1}+1-\frac{p}{2\gamma-1},x\bigg).$$

Proposition 5.2. *Let $\gamma > 1$. For $p < 2\gamma - 1$ we have*

$$\mathbf{E}^\pi\{X_t^p\} = \begin{cases} \displaystyle\bigg(\frac{\sigma^2(2\gamma-1)}{2\alpha}\bigg)^{-p/(2\gamma-1)}\frac{M(p)}{M(0)} & \text{if } \alpha>0 \text{ and } \beta\in\mathbb{R}, \\ \displaystyle\bigg(\frac{\sigma^2(\gamma-1)}{\beta}\bigg)^{-p/(2\gamma-2)}\Gamma\bigg(\frac{2\gamma-1-p}{2\gamma-2}\bigg)\bigg/\Gamma\bigg(\frac{2\gamma-1}{2\gamma-2}\bigg) & \text{if } \alpha=0 \text{ and } \beta>0, \end{cases} \tag{5.5}$$

while $\mathbf{E}^\pi\{X_t\} = \infty$ for $p \geq 2\gamma - 1$. The stationary distribution is given by

$$\mathbf{P}^\pi\{X_t > x\} = \begin{cases} \displaystyle\frac{1}{M(0)}M\bigg(0,\frac{2\alpha}{\sigma^2(2\gamma-1)}x^{1-2\gamma}\bigg) & \text{if } \alpha>0 \text{ and } \beta\in\mathbb{R}, \\ \displaystyle\Gamma\bigg(\frac{2\gamma-1}{2\gamma-2},\frac{\beta}{\sigma^2(\gamma-1)}x^{2-2\gamma}\bigg)\bigg/\Gamma\bigg(\frac{2\gamma-1}{2\gamma-2}\bigg) & \text{if } \alpha=0 \text{ and } \beta>0. \end{cases}$$

Proof. A non-normalized stationary density function is given by the speed measure

$$\frac{dm(x)}{dx} = 2\,x^{-2\gamma}\exp\bigg\{\frac{2\alpha}{\sigma^2(1-2\gamma)}x^{1-2\gamma} - \frac{\beta}{\sigma^2(\gamma-1)}x^{2-2\gamma}\bigg\},$$

so that $\int_0^\infty x^p\,dm(x) = \infty$ for $p \geq 2\gamma - 1$. We readily get the upper case in (5.5) from

$$\begin{aligned} &\int_0^\infty x^p\,dm(x) \\ &= \int_0^\infty 2\,x^{p-2\gamma}\exp\bigg\{\frac{2\alpha}{\sigma^2(1-2\gamma)}x^{1-2\gamma} - \frac{\beta}{\sigma^2(\gamma-1)}x^{2-2\gamma}\bigg\}\,dx \\ &= \frac{2}{2\gamma-1}\int_0^\infty y^{p/(1-2\gamma)}\exp\bigg\{\frac{2\alpha}{\sigma^2(1-2\gamma)}y\bigg\}\sum_{k=0}^\infty\frac{1}{k!}\bigg(\frac{-\beta}{\sigma^2(\gamma-1)}y^{(2-2\gamma)/(1-2\gamma)}\bigg)^k dy, \end{aligned}$$

and along the same lines, the lower case from

$$\int_0^\infty x^p\, dm(x) = \int_0^\infty 2\, x^{p-2\gamma} \exp\left\{ \frac{-\beta}{\sigma^2(\gamma-1)} x^{2-2\gamma} \right\} dx.$$

In the same fashion we calculate the stationary distribution function. □

Proposition 5.3. *Let $\gamma > 1$. We have*

$$\mathbf{E}^\pi\{X_t\} \in (0, -\alpha/\beta) \quad \textit{for } \beta < 0. \tag{5.6}$$

Further, for $\alpha > 0$ and $\beta \in \mathbb{R}$ we have

$$\lim_{\gamma\downarrow 1} \mathbf{E}^\pi\{X_t\} = \begin{cases} -\alpha/\beta & \textit{if } \beta<0 \\ \infty & \textit{if } \beta\geq 0 \end{cases} \quad \textit{and} \quad \lim_{\gamma\to\infty} \mathbf{E}^\pi\{X_t\} = \begin{cases} -\alpha/\beta & \textit{if } \beta<-\alpha \\ 1 & \textit{if } \beta\geq -\alpha \end{cases}, \tag{5.7}$$

while for $\alpha = 0$ and $\beta > 0$

$$\lim_{\gamma\downarrow 1} \mathbf{E}^\pi\{X_t\} = \begin{cases} \infty & \textit{if } \sigma^2 < 2\beta\, e \\ 0 & \textit{if } \sigma^2 \geq 2\beta\, e \end{cases} \quad \textit{and} \quad \lim_{\gamma\to\infty} \mathbf{E}^\pi\{X_t\} = 1. \tag{5.8}$$

Proof. By routine calculations, we have

$$\begin{aligned} M(1) &= \sum_{k=0}^\infty \frac{1}{k!} \left[\frac{-\beta}{\sigma^2(\gamma-1)} \left(\frac{\sigma^2(2\gamma-1)}{2\alpha} \right)^{(2\gamma-2)/(2\gamma-1)} \right]^k \Gamma\left((k+1) \frac{2\gamma-2}{2\gamma-1} \right), \\ M(0) &= 1 + \sum_{k=1}^\infty \frac{1}{(k-1)!} \left[\frac{-\beta}{\sigma^2(\gamma-1)} \left(\frac{\sigma^2(2\gamma-1)}{2\alpha} \right)^{(2\gamma-2)/(2\gamma-1)} \right]^k \left(\frac{2\gamma-2}{2\gamma-1} \right) \Gamma\left(k \frac{2\gamma-2}{2\gamma-1} \right). \end{aligned} \tag{5.9}$$

From this in turn, we readily obtain

$$M(0) = 1 - \frac{\beta}{\alpha} \left(\frac{\sigma^2(2\gamma-1)}{2\alpha} \right)^{-1/(2\gamma-1)} M(1).$$

Combining this with (5.5), we readily get (5.6) from

$$\mathbf{E}^\pi\{X_t\} = 1 \Big/ \left[\left(\frac{\sigma^2(2\gamma-1)}{2\alpha} \right)^{1/(2\gamma-1)} \frac{1}{M(1)} - \frac{\beta}{\alpha} \right]. \tag{5.10}$$

To prove (5.7) for $\beta < 0$ and $\gamma \downarrow 1$, by (5.10), it is enough to show that $\lim_{\gamma\downarrow 1} M(1) = \infty$. This in turn follows by inspection of the following version of (5.9):

$$M(1) = \sum_{k=0}^\infty \frac{1}{(k+1)!} \left[\frac{-\beta}{\sigma^2(\gamma-1)} \left(\frac{\sigma^2(2\gamma-1)}{2\alpha} \right)^{(2\gamma-2)/(2\gamma-1)} \right]^k \left(\frac{2\gamma-1}{2\gamma-2} \right) \Gamma\left((k+1) \frac{2\gamma-2}{2\gamma-1} + 1 \right).$$

To prove (5.7) for $\alpha > 0$, $\beta < -\alpha$ and $\gamma \to \infty$, by (5.10), it is enough to show that $\lim_{\gamma\to\infty} M(1) = \infty$. This in turn follows from the fact that, by routine calculations, term number k in the sum for $M(1)$ in (5.9) converges to $(-\beta/\alpha)^k$ as $\gamma \to \infty$.

To prove (5.7) for $\alpha > 0$, $\beta \geq 0$ and $\gamma \downarrow 1$, notice that $\mathbf{E}^\pi\{X_t\}$ is an non-decreasing function of α and β, by inspection of (4.7). And so it is enough to show $\lim_{\gamma\downarrow 1} \mathbf{E}^\pi\{X_t\} = \infty$ for $\beta = 0$. This in turn we get observing, by (5.5),

$$\mathbf{E}^\pi\{X_t\} = \left(\frac{\sigma^2(2\gamma-1)}{2\alpha}\right)^{-1/(2\gamma-1)} \Gamma\left(\frac{2\gamma-2}{2\gamma-1}\right) \quad \text{for } \alpha > 0 \text{ and } \beta = 0.$$

To prove (5.7) for $\alpha > 0$, $-\alpha \leq \beta < \alpha$ and $\gamma \to \infty$, it is enough to consider $-\alpha < \beta < \alpha$, by the monotonicity noted in the previous paragraph. This in turn we get from (5.10) and that term number k in the sum $M(1)$ goes to $(-\beta/\alpha)^k$ as $\gamma \to \infty$.

The fact that (5.7) holds for $\alpha > 0$, $\beta \geq \alpha$ and $\gamma \to \infty$ follows from (5.8): This is so because when we start with $\lim_{\gamma\to\infty} \mathbf{E}^\pi\{X_t\} = 1$ for $\alpha = 0$ and $\beta > 0$, and succesively increase α, by the noted monotonicity property together with (5.7) for $\alpha > 0$, $\beta < \alpha$ and $\gamma \to \infty$, we must have $\lim_{\gamma\to\infty} \mathbf{E}^\pi\{X_t\} = 1$ for all intermediate $\alpha \in [0, \beta]$.

It remains to prove (5.8). Here the limit when $\gamma \to \infty$ is immediate from (5.5), while the limit when $\gamma \downarrow 1$ follows from (5.5) together with Stirling's formula. □

As $\mathbf{E}^\pi\{X_t\} < -\alpha/\beta$ for $\alpha > 0$, $\beta < 0$ and $\gamma > 1$, Chan, Koralyi, Longstaff and Sanders (1992), Equation 2, misspecified the first moment conditions for their generalized method of moments approach: The reason is that they overlooked the *vis*.

Corollary 5.1. *Let $\gamma > 1$. We have*

$$\mathbf{E}^\pi\left\{\sigma \int_0^t X_s^\gamma dW_s\right\} = -\left(\alpha + \beta \int_0^\infty x\, d\pi(x)\right) t \equiv -d(\alpha, \beta, \sigma, \gamma)t, \tag{5.11}$$

where $d(\alpha, \beta, \sigma, \gamma) > 0$. Further, for $\alpha > 0$ and $\beta \in \mathbb{R}$ we have

$$\lim_{\gamma\downarrow 1} d(\alpha, \beta, \sigma, \gamma) = \begin{cases} 0 & \text{if } \beta < 0 \\ \infty & \text{if } \beta \geq 0 \end{cases} \quad \text{and} \quad \lim_{\gamma\to\infty} d(\alpha, \beta, \sigma, \gamma) = \begin{cases} 0 & \text{if } \beta < -\alpha \\ \alpha+\beta & \text{if } \beta \geq -\alpha \end{cases},$$

while for $\alpha = 0$ and $\beta > 0$

$$\lim_{\gamma\downarrow 1} d(\alpha, \beta, \sigma, \gamma) = \begin{cases} \infty & \text{if } \sigma^2 < 2\beta\, e \\ 0 & \text{if } \sigma^2 \geq 2\beta\, e \end{cases} \quad \text{and} \quad \lim_{\gamma\to\infty} d(\alpha, \beta, \sigma, \gamma) = \beta.$$

Conley, Hansen, Luttmer and Scheinkman (1997), p. 529, claim that a diffusion with a (positive) *vis* at infinity behaves, for large values, as a Brownian motion. But,

for the CKLS model the scale function diminishes all the obtained large values when transforming back from the naturale scaled version, so that the process is different from the Brownian motion. And even if the local martingale is unbiased towards the direction, the speed of the clock will introduce a mean reverting bias. Thus, Conley, Hansen, Luttmer and Scheinkman (1997) give a misleading interpretation of *vis*.

Since we have an entrance *vis* boundary at infinity, the local martingale $\sigma \int_0^t X_s^\gamma \, dW_s$ will induce mean reversion for large values of the process, but display martingale behavior for smaller values, giving it a decreasing mean. For $\beta < 0$ the mean reversion comes from both *vis* and the drift. This is the reason that the stationary mean is always less than $-\alpha/\beta$. The value $d(\alpha, \beta, \sigma, \gamma)$ of the drift of the local martingale in (5.11) measures the size of the *vis*.

5.2. Strong approximations and simulations of the CKLS model

For $\gamma \leq 1$, the arguments of Propositon 7.1 below give strong uniform convergence of the Euler scheme. For $\gamma > 1$, the Euler scheme breaks down with positive probability, by Proposition 4.1. For example, for $\gamma = 50$, the scheme breaks down almost immediately with $\Delta = 10^{-9}$.

Broze, Scaillet and Zakoïan (1995), pp. 220-221, prove that $\mathbf{P}\{Y_n^2 \to \infty\} > 0$ for $\gamma > 1$. We think their proof contains an error: As a first step, they show that

$$\mathbf{P}\{Y_{n+1}^2 \geq (\phi + 1) Y_n^2 \mid Y_n^2\} \geq 1 - d > 0 \quad \text{for } |Y_n| > M, \tag{5.12}$$

for some constants $M, \phi, d > 0$. To finish the proof, they claim that (5.12) and Petruccelli and Woolford (1984), p. 274, give $\mathbf{P}\{\lim_{n\to\infty} Y_n^2 = \infty | Y_0\} > 0$.

Working through the details in Petruccelli and Woolford (1984), p. 274, the inequality

$$\mathbf{P}\{Y_{n+1}^2 \geq (\phi + 1) Y_n^2 \mid Y_n^2\} \geq 1 - c/Y_n^2 = 1 - d_n > 0 \quad \text{for } |Y_n| > M, \tag{5.13}$$

for some constant $c > 0$ (for a different model), is used to get the claimed convergence. However, the requirement in (5.13) is stronger than the requirement in (5.12)!

We now examine implicit Euler schemes for the CKLS model, see (4.1). As the non-Lipschitz part of the CKLS model is the volatility (not the drift), we need an implicit scheme ($\theta_\sigma > 0$). The explicit part of the implicit scheme for the CKLS model is

$${}_x\tilde{Y}_n = {}_xY_n + (1 - \theta_b)(\alpha + \beta {}_xY_n - \theta_\sigma \gamma \sigma^2 {}_xY_n^{2\gamma - 1})\Delta + (1 - \theta_\sigma)\sigma {}_xY_n^\gamma \Delta W_n,$$

and the non-linear equation to be solved for the implicit part is $f({}_xY_{n+1}) = {}_x\tilde{Y}_n$, where

$$f(y) = y - \theta_b(\alpha + \beta y - \theta_\sigma \gamma \sigma^2 y^{2\gamma - 1})\Delta - \theta_\sigma \sigma y^\gamma \Delta W_n$$

(with x referring to the initial value). The issue whether $f(Y_{n+1}) = \tilde{Y}_n$ has a unique solution Y_{n+1} depends on the size of ΔW_n: The derivative f' has global minimum at

$$\bar{y} = \left[\frac{\Delta W_n}{2\theta_b\sigma(2\gamma-1)\Delta}\right]^{1/(\gamma-1)} \quad \text{with} \quad f'(\bar{y}) = 1 - \theta_b\beta\Delta - \frac{\theta_\sigma\gamma}{4\theta_b(2\gamma-1)}\frac{(\Delta W)^2}{\Delta}.$$

The two roots $r_\pm$, $r_- < r_+$, are given by

$$r_\pm = \left[\frac{\Delta W_n \pm \sqrt{d}}{2\theta_b\sigma(2\gamma-1)\Delta}\right]^{1/(\gamma-1)} \quad \text{where} \quad d = (\Delta W_n)^2 - 4(1-\theta_b\beta\Delta)\frac{\theta_b(2\gamma-1)}{\theta_\sigma\gamma}\Delta. \tag{5.14}$$

If $\theta_b\beta\Delta < 1$ and the discriminant is positive, then the roots $r_\pm$ are both positive [negative] if $\Delta W_n > 0$ [$\Delta W_n < 0$].

The asymptotic probability that f is not monotone is $\mathbf{P}\{\mathrm{N}(0,1) > 2\sqrt{\theta_b(2\gamma-1)/(\theta_\sigma\gamma)}\}$ as $\Delta \downarrow 0$. With $\theta_b = \theta_\sigma = 1$ and γ close to one, that probability is 2.3%, decreasing to 0.23% for large values of γ. For f not monotone, there are several options.

We suggest the following: If f is not monotone, then for $Y_n \in [f(r_+), f(r_-)]$ the solution $f(Y_{n+1}) = Y_n$ is not unique. To have the continuity $\tilde{Y}_{n+1} \to Y_{n+1}$ as $\tilde{Y}_n \to Y_n$, we must select the smallest of the possible solutions. One option is to use the full implicit scheme for $Y_n < f(r_+)$, where the solution is unique. Another option is to use the full implicit scheme for $Y_n < f(r_-)$, and in cases of more than one solution choose the smallest one. The motivation is that the solution of an SDE in the interval $[t_n, t_{n+1}]$ should depend only on the Brownian motion in the interval, together with the drift and volatility at X_{t_n}, so that this information should suffice to determine $X_{t_{n+1}}$.

The question remains what to do if $Y_n > f(r_+)$ [$Y_n > f(r_-)$]. We suggest that θ_b and θ_σ are adjusted so that $f(Y_{n+1}) = Y_n$ gets a unique solution. The simplest choice is to take an explicit step ($\theta_b = \theta_\sigma = 0$).

In our test examples, the explicit step is applied very seldom, and only if $\Delta W_n > 0$ is large, at the same time as $Y_n > f(r_\pm)$. In practice we get a stable numerical scheme, even for very large values of γ.

We now describe yet another and fruitful approach to simulate the CKLS model, which is to simulate the transformed process (5.2). With a constant volatility the implicit schemes of interest reduce to the theta method; and for $\theta_b = 1$ the BE scheme,

$${}_z\tilde{Y}_n = {}_zY_n + (1-\theta_b)\varphi({}_zY_n)\Delta + \sigma(1-\gamma)\Delta W_n,$$

where φ is defined in equation (5.3). The non-linear equation to be solved is $g({}_zY_{n+1}) = {}_z\tilde{Y}_n$ where $g(z) = z - \theta_b\varphi(z)\Delta$. As $g : (0,\infty) \to (-\infty,\infty)$ invertible, the BE scheme defines a solution which can attain any positive value, exactly like the true solution.

The full implicit scheme is promising as the function φ in (5.3) is C^1 and one-sided Lipschitz. Since b has a polynomial behaviour at infinity, Mattingly, Stuart and Higham (2002), Theorem 5.3, shows that for the true solution and the continuous-time extension of the BE approximation, all moments of order $p > 2$ are uniformly bounded, and the approximation converges uniformly in L^2 with order $\frac{1}{2}$. By transforming back with the inverse function $f^{-1}({}_zY_n)$, $f^{-1}(y) = y^{1/(1-\gamma)}$ which is decreasing and convex, we get our benchmark for the true solution sample path of the CKLS model.

We will now consider some numerical examples of CKLS models.

In Figure 1 in Appendix A, the left panel shows the stationary mean as a function of $\gamma > 1$, in part illustrating the limit behavior from Proposition 5.3, while the right panel shows the stationary density for two sets of parameter values.

We illustrate the results from Corollary 5.1 in Figure 2.

Another way to measure the reversion back to the stationary level is by the spectral gap. Genon-Catalot, Jeantheau and Larédo (2000) give the upper bound $1/(8Cm((0, \infty))^2)$ for that gap, where C is the median of π. With the same parameters as in Figure 1, we display this bound in Figure 3.

Even though the gap estimate may be crude, it shows strong exponential mean reversion for large values of γ. The reversion grows with β. As the stationary density moves to the right when β increases, this suggests that excursions from the mean become higher and shorter, like peaks.

Sample paths are different for the cases $\gamma < 1$ and $\gamma > 1$: For $\gamma > 1$ the process escapes the mean during short explosive peaks, while for $\gamma < 1$, the clock is slower.

Simulation of the CKLS model using the transformation (5.2). We now give two numerical examples of the CKLS model with $\gamma = 50$, giving an extremely high *vis*. The other parameters are $\alpha = 1$, $\beta = \pm 1$ and $\sigma = 2$, to illustrate the difference between pure *vis* ($\beta = 1$) and a diffusion with stationarity from both *vis* and drift ($\beta = -1$).

In Figure 4 the left panels show two sample paths of the CKLS model using the full implicit Euler scheme ${}_zY_n$), with $X_0 = 1$ and $\Delta = 10^{-9}$, and transformed back to the CKLS model, see (5.2). Note that for $\beta = 1$ the process has a lot of peaks. Both processes are reverting extremely fast back to the stationary level. The transformed processes (5.2) are plotted in the right panels, and they behave wildly!

The peaks for the processes in Figure 4 are very narrow. To see the behavior at peaks, we display two windows with volatile periods in Figure 5. Note that the excursions from the mean are very short. Also, the process in the right panel ($\beta = -1$) has a longer excursion than the one in the left panel ($\beta = 1$). This is the general picture, and is also confirmed by estimates for the spectral gap in Figure 3.

Albeit the simulation scheme converges as $\Delta \downarrow 0$, the CKLS model is hard to simulate for large γ. In contrast to the explicit scheme, which overestimates the peaks and ends up transient, the implicit scheme underestimates peaks, giving a downward bias. For example, the peaks close to 1.15 in Figure 5 reduce to 1.07 for the step size 10^{-5}.

Simulation of the CKLS model using modified implicit schemes. Consider the difference between a modified full implicit scheme $({}_xY_n)$ and the transformed scheme $f^{-1}({}_zY_n)$. The full implicit scheme for the transformed process converges by Higham, Mao and Stuart (2002).

We trust the Euler approximation $({}_zY_n)$ and define the relative error for a modified implicit Euler scheme, $({}_xY_n)$, as the relative difference between the two implicit Euler schemes

$$\varepsilon_n = 2\frac{f^{-1}({}_zY_n) - {}_xY_n}{f^{-1}({}_zY_n) + {}_xY_n}, \quad n = 0, 1, \ldots, \qquad f^{-1}(z) = z^{\frac{1}{1-\gamma}}.$$

Note that $\varepsilon_0 = 0$ and that $\varepsilon_n > 0$ when a modified full implicit Euler scheme ${}_xY_n$ underestimates the true value. In most cases, the two schemes attain their extremes at the same times, but in rare cases there are differences.

We used the modified full implicit scheme with the left root. And so, for ${}_xY_n \leq f(r_-)$ we use the full implicit Euler scheme, while otherwise we take an explicit step.

The right panel of Figure 6 shows the relative error ε_n for $\beta = -1$. Remarkably, we did not take any explicit steps. Large errors arise around high peaks, when the transformed process $({}_zY_n)$ is close to zero. Otherwise, the error is of magnitude 10^{-6}.

The left panel in Figure 6 shows $\beta = 1$. The bracketed numbers indicate the numbers of explicit steps applied around peaks. Except for at peaks, the relative error ε_n is about 10^{-6}, just as for $\beta = -1$. To illustrate this, we have in Figure 7 divided $[0, 1]$ into 1000 equally long subintervals, and evaluated the ε_n only at the largest value of the process in each subinterval. The figure is very similar to Figure 6.

To give a better picture of the problem around the peaks we have plotted the error process (ε_n) in Figure 8 with the same window as in Figure 5.

We may instead take explicit steps whenever ${}_xY_n$ is larger than $f(r_+)$, using $f(r_+)$ as the boundary for where to take implicit and explicit steps. This will not improve this significantly. The error using the root r_+ is plotted in the left panel of Figure 9.

Instead of full explicit steps, we could take $\theta_b = 1$ and $\theta_\sigma < 1$, still using $f(r_+)$ as the boundary for where to stop with implicit steps. For a "troubled" increments ΔW_n, we choose a θ_σ such that the discriminant is negative, see (5.14). Specifically, we take

$$\theta_b = 1 \quad \text{and} \quad \theta_\sigma = \frac{2(1 - \theta_b\beta\Delta)\theta_b(2\gamma - 1)\Delta}{\gamma(\Delta W_n)^2}.$$

For this θ_σ, the discriminant in (5.14) is zero for $d = 2\theta_\sigma$, while positive for $\theta_\sigma = 1$. Hence $\theta_\sigma \in (0, 1)$. The right panel of Figure 9 shows the relative error for the scheme.

All schemes seems to differ at the peaks, because at peaks the clock is so fast that, even with step size 10^{-9}, the process can change value up to 0.03 for a single step.

The case of Chan, Koralyi, Longstaff and Sanders (1992). As a last example we use the parameters from the paper by Chan, Koralyi, Longstaff and Sanders (1992),

$$\alpha = 0.0408,\ \beta = -0.5921,\ \sigma^2 = 1.6704,\ \gamma = 1.4999. \tag{5.15}$$

The data set in Chan, Koralyi, Longstaff and Sanders (1992) is the monthly yields of U.S. one-month Treasury Bills, 1964-89 (CRSP). They view the data as discretely observed data from the CKLS model, hence $\Delta = \frac{1}{12}$. The stationary mean is 0.06886 and $-\alpha/\beta = 0.06891$, so the true mean is in this case only slightly smaller than if no *vis* was present. Still this SDE displays different behavior than for the case $\frac{1}{2} \le \gamma < 1$.

In Figure 10 we have plotted the CKLS model (5.15) for 25 years (left panel) and 1000 years (right panel), with the latter showing the high peak characteristics of *vis*.

We decompose the process X into its drift part $X_0 + \int_0^t (\alpha + \beta X_s)\, ds$ and local martingale part $\sigma \int_0^t X_s^\gamma\, dW_s$. We start by simulating X_t as in Figure 10. Next we simulate the drift part and the local martingale part as

$$\int_{t_n}^{t_{n+1}} (\alpha + \beta X_s)\, ds \approx \alpha\Delta + \frac{\beta}{2}(X_{t_{n+1}} + X_{t_n})\Delta, \tag{5.16}$$

$$\sigma \int_{t_n}^{t_{n+1}} X_s^\gamma\, dW_s \approx X_{t_{n+1}} - X_{t_n} - \alpha\Delta - \frac{\beta}{2}(X_{t_{n+1}} + X_{t_n})\Delta. \tag{5.17}$$

If no *vis* effect were present, the local martingale part should have had zero mean, so that (5.16) and (5.17) were zero mean processes, under the stationary measure.

Figure 11 shows the drift and local martingale parts of the SDE started at 0.06886 (left panel), and the drift and the local martingal parts together with the solution started at 4, but moved different constant steps in the y direction to facilitate viewing (right panel). Note that the negative drift of the local martingale is recognizable only when the process is much larger than the stationary mean.

As long as the process is close to the stationary mean there is no recognizable drift effect (left panel of Figure 11) and hence, close to the mean, the reversion is controlled by the drift. In other words, the *vis* effect is only present for large values. As discussed earlier this is the case when β is dominating, $\beta < -\alpha$, which is the case here.

Endnotes for the CKLS example. To show that our numerical schemes capture the drift in the local martingale (5.17), we have included the new parameter set $\alpha = 1$, $\beta = 1$, $\sigma = 2$, and $\gamma = \frac{3}{2}$, with stationary mean 3.13 and *vis* effect $d(\alpha, \beta, \sigma, \gamma) = 4.13$.

Figure 12 displays the process with its local martingale and drift components. Since $\beta > 0$ there is no reversion from the drift. The stationary local martingale has mean $-4.13t$. For Figure 11 we argued that there is a close connection between peaks of the local martingale and of the process: Figure 12 shows an almost perfect match!

6. A hyperbolic diffusion with *vis*

Our second example is within the hyperbolic class of diffusions, see Bibby and Sørensen (2003). The actual SDE we study is taken from Bibby and Sørensen (1997):

$$dX_t = \sigma \exp\Big\{\frac{1}{2}\Big(\alpha\sqrt{\delta^2 + (X_t - \mu)^2} - \beta(X_t - \mu)\Big)\Big\}\, dW_t, \quad X_0 = \zeta.$$

To satisfy Assumptions 2.1 and 2.3 the parameters must satisfy $\alpha > |\beta| \geq 0$, $\delta, \sigma > 0$ and $\mu \in \mathbb{R}$. Then the diffusion is also ρ-mixing, as $\pm\infty$ are entrance boundaries, see Hansen, Scheinkman and Touzi (1998), Section 4. There is a high degree of *vis*

The stationary solution has all moments, some of which are calculated by Bibby and Sørensen (2003). The stationary density is maximal at $\mu + \delta\beta/\sqrt{\alpha^2 - \beta^2}$.

As in Example 3.2, the stationary local martingale is uniformly integrable but not a martingale.

Denoting the spectral gap λ, ergodicity and ρ-mixing gives $\mathbf{E}^x\{\int_0^t \sigma(X_s)\, dW_s\} = O(e^{\lambda t})$ as $t \to \infty$ for $x \in \mathbb{R}$, while $\mathbf{E}^\tau\{\int_0^t \sigma(X_s)\, dW_s\} = 0$. Hence mean reversion is not due to bias of the local martingale, but that the clock is very quick at large values.

6.1. Time-changed simulation

By Corollary 4.1, the Euler scheme is transient with positive probability. This should then apply also to higher order explicit schemes, and from numerical tests we have seen that the Milstein and strong 1.5 schemes start to oscillate between large positive and negative values. However, Bibby and Sørensen (1997) report that the strong 1.5 scheme works for them!

The implicit scheme is problematic because the equation to be solved will not have a unique solution. The transformation method that was used for the CKLS model is not an option here, as the function f in (4.7) and its inverse have to be evaluated by time-consuming numerical methods, and the drift in (4.7) is not one-sided Lipschitz.

We will describe an alternative way to simulate a local martingale as a time-changed Brownian motion, which will be refered to as *time-changed simulation*. First we set up some notation (see e.g., Revuz and Yor, 1999, Chapter 5):

Let $[X]_t = \int_0^t \sigma^2(X_s)\,ds$ be the quadratic variation process. If T_t solves $[X]_{T_t} = t$, then $B_t = X_{T_t} - X_0$ is a Brownian motion: The idea is to simulate B and get X from

$$T_t = \int_0^t \frac{du}{\sigma^2(X_0 + B_u)} \quad \text{and} \quad X_{T_t} = X_0 + B_t.$$

Consider a grid $0 = t_0 < t_1 < \ldots < t_N = T$ with spacing Δ. Given T_{t_n}, we have

$$X_{T_{t_{n+1}}} = X_0 + B_{t_{n+1}} \quad \text{where} \quad T_{t_{n+1}} - T_{t_n} = \int_{t_n}^{t_{n+1}} \frac{du}{\sigma^2(X_0 + B_u)}. \tag{6.1}$$

For B close to the boundaries the speed measure gets small, so that $T_{t_{n+1}} - T_{t_n}$ is very small, which makes computations slow. We will now explain how to deal with this:

Pick intervals $(a_1, b_1) \subsetneq (a_2, b_2)$ and numbers $\varepsilon_1 > \varepsilon_2 > 0$ such that $\sigma^2(x)$ is strictly monotone outside (a_1, b_1) with $1/\sigma^2(a_1) = 1/\sigma^2(b_1) = \varepsilon_1$ and $1/\sigma^2(a_2) = 1/\sigma^2(b_2) = \varepsilon_2$. As long as $B_{t_n} \in (a_2 - X_0, b_2 - X_0)$ we calculate $X_{T_{t_{n+1}}}$ by (6.1). If B reaches the bound $a_2 - X_0$ $[b_2 - X_0]$ at the time $\tau = t_i$, then we stop the scheme (6.1) and start it again at the first time $\rho = t_j$ at which B returns to the bound $a_1 - X_0$ $[b_1 - X_0]$.

To approximate the integrals in (6.1), we use a trapezoid rule for regular steps from t_n to t_{n+1}, and for jumps with $\rho - \tau \leq 1$. For larger jumps we use a grid with spacing $\tilde{\Delta} = 0.1$. As we know the values of the Brownian motion at the endpoints, we simulate intermediate values according to a (time-scaled) Brownian bridge.

By the strong *vis*, the hyperbolic diffusion spends very little time at numerically large values, so that the excursions in (T_τ, T_ρ) should not influence "overall properties" of the solution significantly. Still, in some applications, these excursions could be important.

6.2. A numerical example

The parameter found by Bibby and Sørensen (1997) for stock price dynamics were

$$\alpha = 4.4875,\ \beta = -3.8412,\ \delta = 1.1949,\ \mu = 7.2915,\ \sigma = \sigma_0 = 0.0047.$$

This gives a stationary distribution with mean 4.1705 and variance 3.8943, which is plotted in the left panel of Figure 13 in Appendix A.

Simulations by the time-change scheme, with $\Delta = 10^{-5}$, $T = 1000$, $\varepsilon_1 = 0.1$, $\varepsilon_2 = 0.01$ and $X_0 = 4.1705$ (the stationary mean) are displayed to the right in Figure 13. There we also considered $\sigma = \sigma_1 = 0.047$, meaning that the clock runs 100 times faster.

7. A family of heavy tailed SDE

Given a constant $a < \frac{1}{3}$, our third SDE is given by

$$dX_t = 3X_t^a\,dt + 3X_t^{2/3}\,dW_t, \quad X_0 = \zeta > 0. \tag{7.1}$$

This SDE satisfies Assumptions 2.1 and 2.3, with speed measure given by

$$\frac{m(x)}{dx} = \frac{2}{9}x^{-4/3}\exp\left\{\frac{2}{3a-1}x^{a-1/3}\right\} \quad \text{for } x > 0. \tag{7.2}$$

The boundary 0 is natural and ∞ a positive *vis* natural boundary. There is no spectral gap, see Hansen, Scheinkman and Touzi (1998), Section 4: The lack of ρ-mixing indicates that the process can in relatively long periods stay away from the stationary level.

Stationary moments of order $p < \frac{1}{3}$ exist, and are easily calulated from (7.2). The local martingale part $\int_0^t 3X_s^{2/3}\,dW_s$ of the stationary solution to (7.1) is not a martingale, because this would contradict stationarity in the following way:

$$\mathbf{E}^\pi\{X_t - X_0\} = \mathbf{E}^\pi\left\{\int_0^t 3X_s^a\,ds + \int_0^t 3X_s^{2/3}\,dW_s\right\} = 3t\int_0^\infty x^a\,d\pi(x) < \infty. \tag{7.3}$$

The stationary density attains its maximum at $x = 2^{3/(3a-1)}$. Notice that the process is pushed towards zero as a increases. Obviously, accurate simulations of (7.1) is an issue of both stability at infinity, and control of the boundary at zero.

7.1. Simulation techniques

Itô-Taylor scemes are strong uniformly convergent under linear growth and Lipschitz drift and volatility, see Kloeden and Platen (1995), Section 10.6. For $a \geq 0$, we can have an Itô- Taylor scheme that is uniformly closer than δ to the true solution, with probability $1 - \delta$, for any $\delta \in (0, 1)$, by using the modified SDE of the proof below, picking $\Delta, \varepsilon > 0$ small enough.

Proposition 7.1. *For $a \geq 0$ the Euler scheme is strong uniformly convergent.*

Proof. By Higham, Mao and Stuart (2002), Theorem 2.2, it is enough to show bounded moments of some order $p > 2$ for suprema of the true solution and the Euler scheme, started at a fixed initial value $\zeta = x$. Replace (7.1) with an SDE with Lipschitz drift and volatility that coincide with the original ones on (ε, ∞), where $\varepsilon \in (0, x)$.

Denoting the solution to the new SDE $\tilde{X}$, and $\tau_\varepsilon = \inf\{t > 0 : X_t = \varepsilon\}$, we have

$$\begin{aligned}
&\mathbf{E}^x\Big\{\sup_{t\in[0,T]} X(t)^p\Big\} \\
&\le \mathbf{E}^x\Big\{\sup_{t\in[0,\tau_\varepsilon]} \tilde{X}(t)^p \mathbf{1}_{\{\tau_\varepsilon<T\}}\Big\} + \mathbf{E}^x\Big\{\sup_{t\in[0,T]} X(t)^p\Big\}\mathbf{P}^x\{\tau_\varepsilon<T\} + \mathbf{E}^x\Big\{\sup_{t\in[0,T]} \tilde{X}(t)^p \mathbf{1}_{\{\tau_\varepsilon\ge T\}}\Big\} \\
&\le \mathbf{E}^x\Big\{\sup_{t\in[0,T]} \tilde{X}(t)^p\Big\} + \mathbf{E}^x\Big\{\sup_{t\in[0,T]} X(t)^p\Big\}\mathbf{P}^x\{\tau_\varepsilon<T\}.
\end{aligned}$$

Since $\mathbf{P}\{\tau_\varepsilon < T\} < 1$, we get the moment bound on X from a bound on $\tilde{X}$. But such a bound, for any $p \ge 2$, is given e.g., in Kloeden and Platen (1995), Exercise 4.5.5.

For the Euler scheme, we can extend the drift and volatility to $(-\infty, 0]$, in any way that does not violate linear growth, to get an Euler scheme Y_n that satisfies

$$Y_{n+1}^2 \le Y_n^2 + C_1\left(1 + Y_n^2\right)\left(\Delta + \Delta W_n + \Delta W_n^2\right) \quad \text{for } \Delta \le 1 \text{ and } n < N,$$

for some constant $C_1 > 0$. And so the submartingale Z_n^2, given by

$$Z_{n+1}^2 = Z_n^2 + C_1\left(1 + Z_n^2\right)\left(\Delta + \Delta W_n + \Delta W_n^2\right) \quad \text{for } n < N, \quad Z_0^2 = x^2,$$

satisfies $Z_n^2 \ge Y_n^2$. As we have, for some constant $C_2 > C_1$,

$$Z_{n+1}^4 \le Z_n^4 + C_2\left(1 + Z_n^4\right)\left(\Delta + \Delta W_n + \Delta W_n^2 + |\Delta W_n|^3 + \Delta W_n^4\right)$$

for $\Delta \le 1$ and $n < N$, we get, for some constant $C_3 > C_2$,

$$\mathbf{E}\{Z_{n+1}^4\} \le \mathbf{E}\{Z_n^4\} + C_3\left(1 + \mathbf{E}\{Z_n^4\}\right)\Delta \quad \text{for } \Delta \le 1 \text{ and } n < N.$$

Hence, by iteration, $\mathbf{E}\{Z_n^4\} \le (1+x^4)(1+C_3\Delta)^n - 1$. Now Doob's maximal inequality gives

$$\begin{aligned}
&\sup_{\Delta>0} \mathbf{E}\Big\{\sup_{n\le N} Y_n^4\Big\} \\
&\le \sup_{\Delta>0} \mathbf{E}\Big\{\sup_{n\le N} Z_n^4\Big\} \le \Big(\frac{4}{3}\Big)^4 \sup_{\Delta>0} \mathbf{E}\{Z_N^4\} \le \Big(\frac{4}{3}\Big)^4 \sup_{\Delta>0}(1+x^4)(1+C_3\Delta)^n < \infty. \quad \square
\end{aligned}$$

For $a < 0$ explicit schemes are unstable, as values close to zero jump to high values from which there is little reversion. For example, for $a = -10$, we have noted instability for $\Delta = 10^{-9}$!

As for the CKLS model, we can use the transformation (4.7), with $f(x) = x^{1/3}$ and $\varphi(z) = z^{3a-2} - z^{-1}$ one-sided Lipschitz, so that $Z_t = f(X_t)$ satisfies

$$dZ_t = \varphi(Z_t)\,dt + dW_t, \quad Z_0 = f(\zeta) > 0. \tag{7.4}$$

With the notation of the CKLS example, the partial explicit step for (7.4) is

$${}_z\tilde{Y}_n = {}_zY_n + (1-\theta_b)\varphi({}_zY_n)\Delta + \Delta W_n.$$

The non-linear equation to be solved is $g({}_zY_{n+1}) = {}_z\tilde{Y}_n$, where $g(z) = z - \theta_b\varphi(z)\Delta$. Then we transform back with $f^{-1}(z) = z^3$, and the approximation of X_{t_n} is ${}_xY_n = f^{-1}({}_zY_n)$. By Higham, Mao and Stuart (2002), this transformation scheme converges to the true solution.

7.2. A numerical example

The left panel in Figure 14 in Appendix A, shows the SDE (7.1) simulated in the interval $[0, 10]$ for $a = -10$, using the BE scheme ($\theta_b = 1$) with $\Delta = 10^{-6}$ and $X_0 = 0.935$ − the maximum of the speed density. Notice the ability to escape from the value 0.935 during long periods. On the other hand, the right panel displays the process in the interval $[8, 10]$, and shows that it also stays close to 0.935 for long periods.

In Figure 15, everything is as in Figure 14, except that $a = \frac{1}{10}$ and the maximum of the speed density is at $X_0 = 0.05127$. Note that the behaviour of the process for large values (the left panel), is virtually identical to that when $a = -10$, illustrating that we have *vis*. On the other hand, the process spends much less time close to the maximum of the speed density, than when $a = -10$ (right panel).

8. Conclusion

We have studied a class of stationary and ergodic SDE, for which stationarity is ensured by a high volatility - *vis*. SDE with *vis* escape from the stationary level often, but in short periods if the *vis* is strong. Between these excursions, the process is very steady. As SDE with stationarity from mean reversion by the drift do not behave in this manner, SDE with *vis* are important additions to more conventional models.

The *vis* appears at the boundaries of the SDE. Either we have a local martingale part of the solutions that is not a martingale, with a mean reverting drift, or we have a martingale or non-martingale local martingale part that is mean reverting, simply because the clock runs quicker nere boundaries. We conclude that interpretations and statistical methods for SDE with *vis* in the literature have to be revised (see below).

To work with SDE with *vis* it is important to have simulation methods. We considered simulated of strong solutions. As virtually all traditional simulation schemes may fail for SDE with *vis*, we considered alternative methods.

We gave three examples of SDE with a different degree of *vis*: The CKLS model has a medium degree of *vis*, where some but not all moments exist, and is or is not ρ-mixing. We simulated CKLS by transformation of the SDE and by modified implicit schemes. An SDE with a stationary distribution in the hyperbolic class is ρ-mixing with a high degree of *vis*, and all moments exist. These SDE were simulated by change of time. The class of heavy tailed SDE were not ρ-mixing, and had a weak *vis* with an infinite stationary mean. They were simulated by transformation of the SDE.

There are mistakes in the literature on inference for SDE with *vis*.

Appendix A. Figures

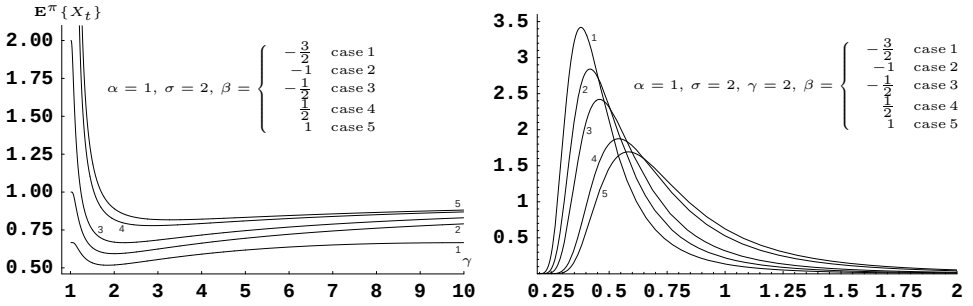

FIGURE 1: The stationary mean as a function of γ and examples of the shape of the stationary density

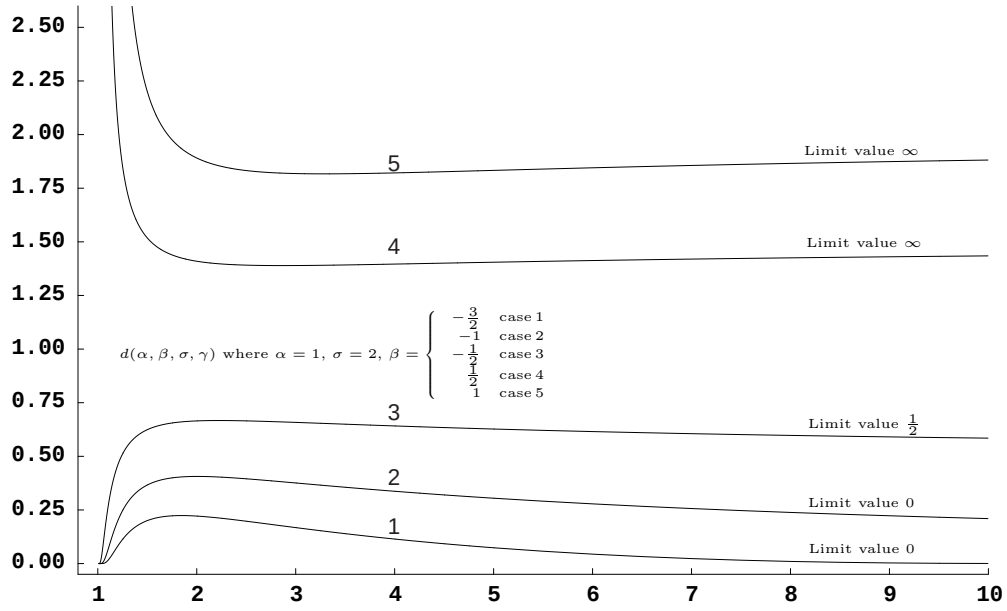

FIGURE 2: Minus the mean, $d(\alpha, \beta, \sigma, \gamma)$, (5.11), of the local martingale, (5.17)

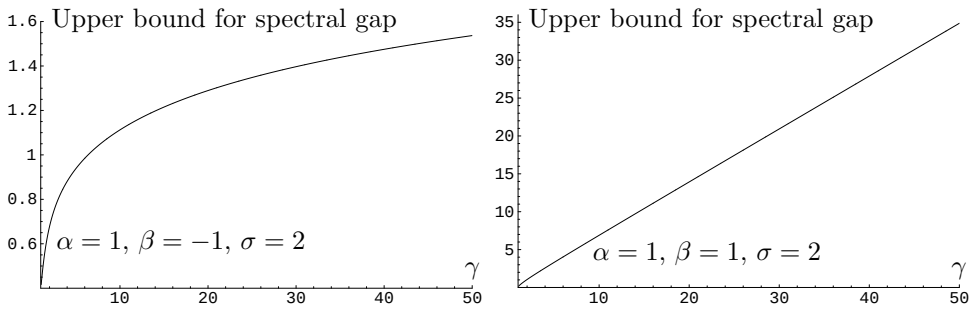

FIGURE 3: A upper bound for the spectral gap in the CKLS model

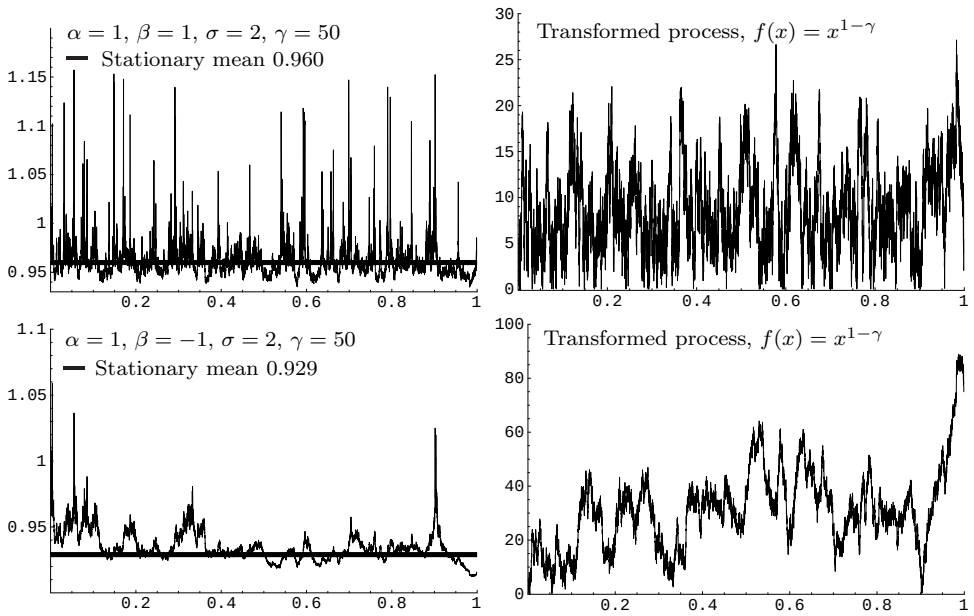

FIGURE 4: The CKLS model with $\Delta = 10^{-9}$ sample paths

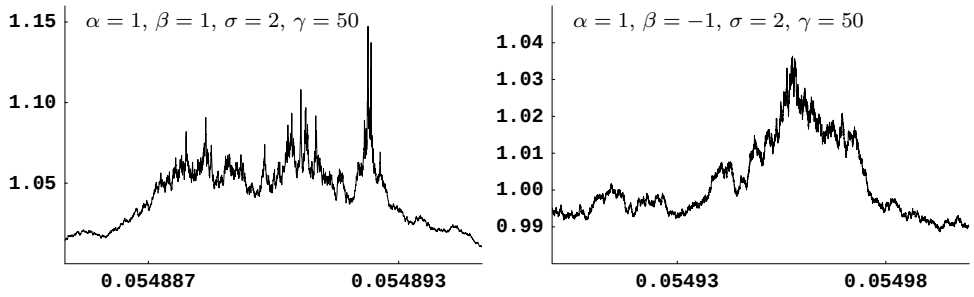

FIGURE 5: Two windows each covering one of the volatile periods for one of the processes in the left panel of Figure 4

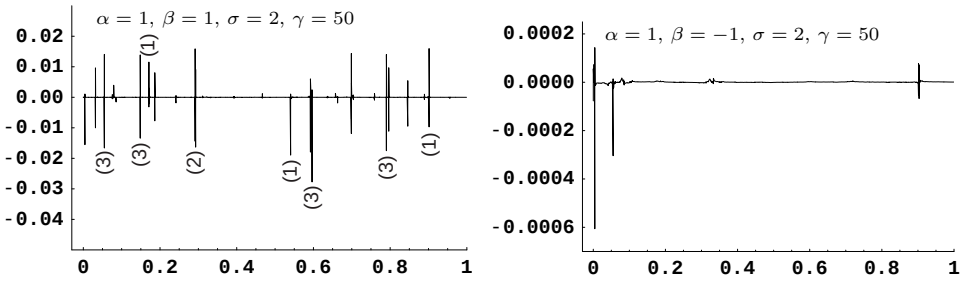

FIGURE 6: The relative error (ε_n) with $\Delta = 10^{-9}$ for the CKLS model, Figure 4

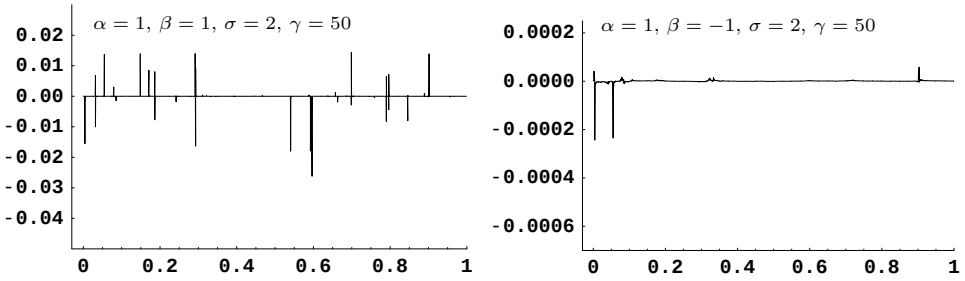

FIGURE 7: (ε_n) evaluated only at the extreme points for each subinterval

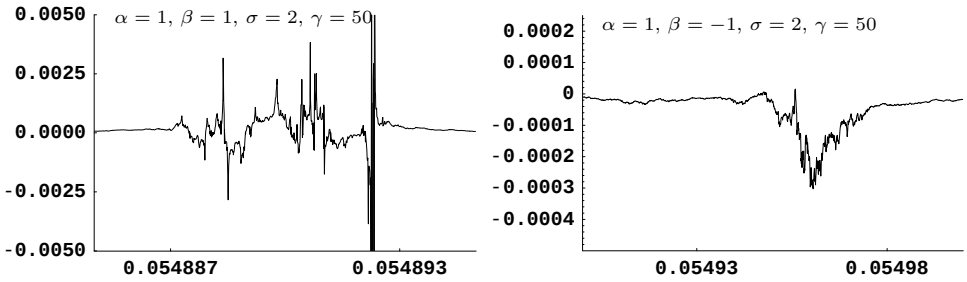

FIGURE 8: (ε_n) for the windows in Figure 5

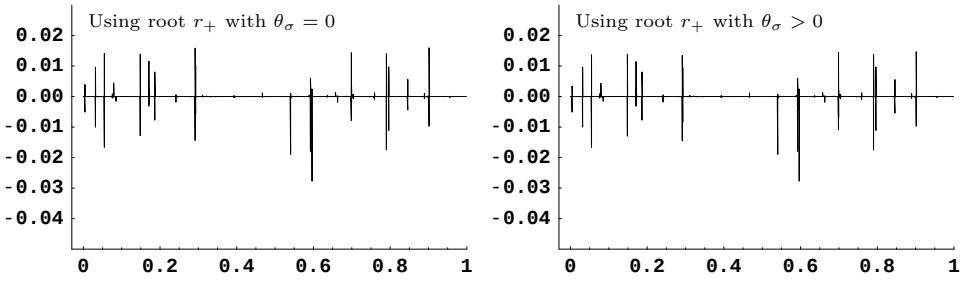

FIGURE 9: The error (ε_n), $\Delta = 10^{-9}$, for two modified schemes

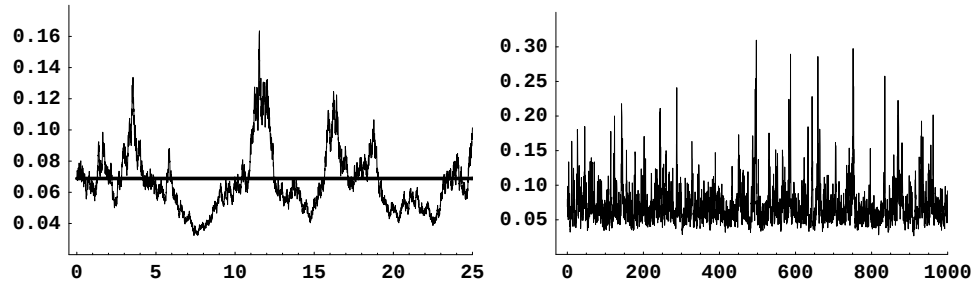

FIGURE 10: The CKLS model, $X_0 = 0.06886$, $\Delta = \frac{1}{12}10^{-5}$

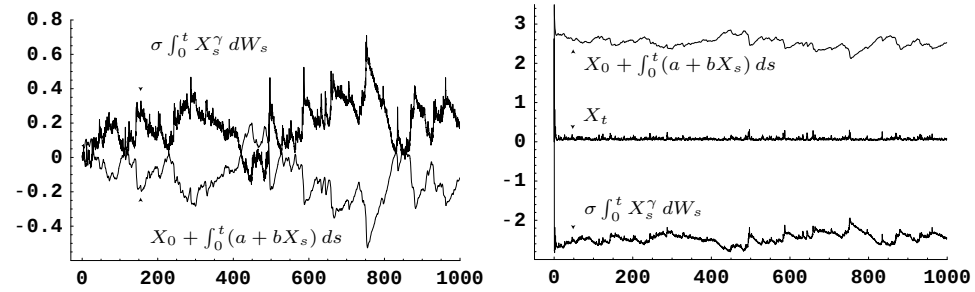

FIGURE 11: Decomposing X_t to its drift part and its local martingale part (5.17) for two initial values $X_0 = 0.06886$ (left panel) and $X_0 = 4$ (right panel)

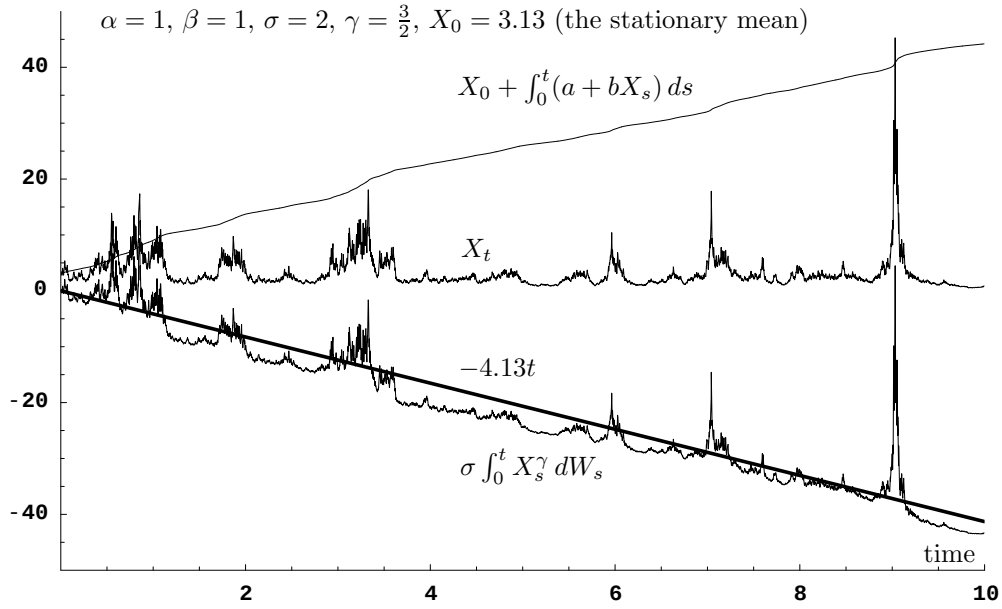

FIGURE 12: Decomposing X_t to its drift part and its local martingale part (5.17)

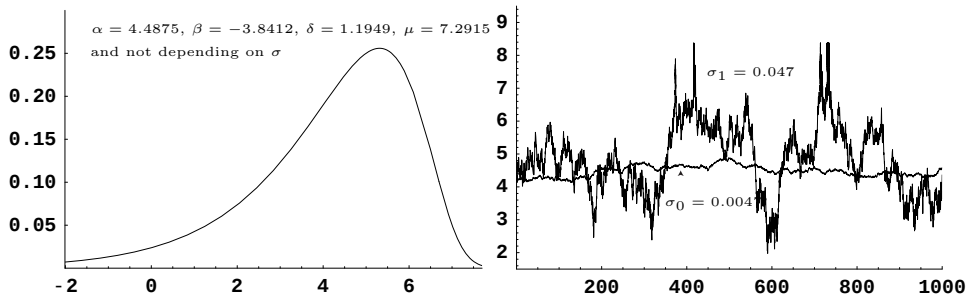

FIGURE 13: Hyperbolic diffusion: The stationary density and two sample paths with different speeds

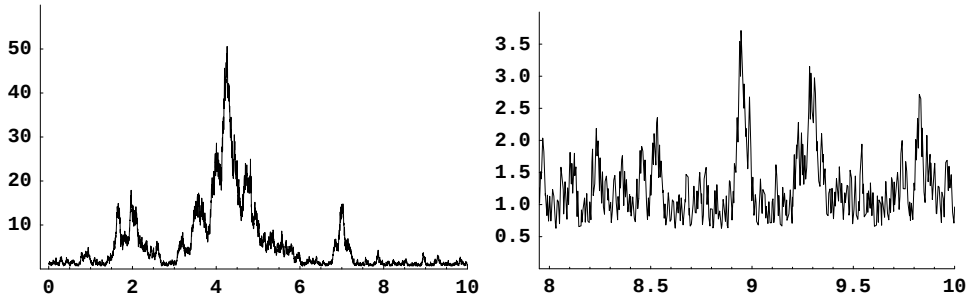

FIGURE 14: Heavy tailed diffusion with $a = -10$, $X_0 = 0.935$ and $\Delta = 10^{-6}$.

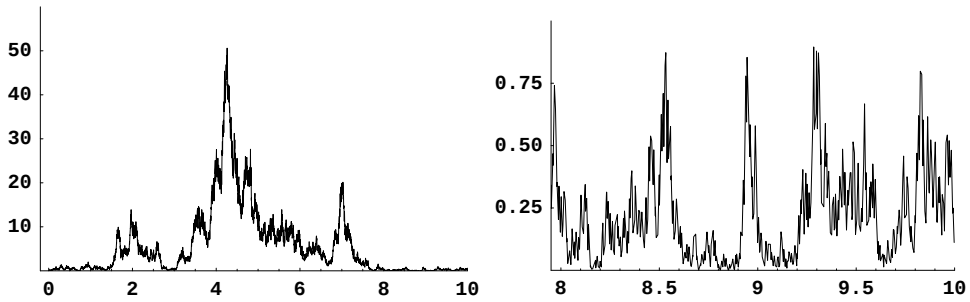

FIGURE 15: Heavy tailed diffusion with $a = \frac{1}{10}$, $X_0 = 0.05127$ and $\Delta = 10^{-6}$.

Acknowledgement

The first author, J.M.P. Albin, was supported by The Swedish Research Council contract no. 621-2003-5214.

The second author, Bjarne Astrup Jensen, gratefully acknowledges financial support from the Danish Social Science Research Council.

References

[1] Arbib, M. A. (1965). Hitting and martingale characterizations of one-dimensional diffusions. *Z. Wahrsch. verw. Gebiete* **4,** 232–247.

[2] Bibby, B. M. and Sørensen, M. (1997). A hyperbolic diffusion model for stock prices. *Finance and Stochastics* **1,** 25–41.

[3] Bibby, B. M. and Sørensen, M. (2003). Hyperbolic processes in finance. In: Rachev, S. T. (ed.) *Handbook of Heavy Tailed Distributions in Finance,* 211–248. Elsevier, New York.

[4] Broze, L., Scaillet, O. and Zakoïan, J.-M. (1995). Testing for continuous-time models of the short-term interest rate. *J. Empirical Finance* **2,** 199–223.

[5] Chan, K., Koralyi, G., Longstaff, F. and Sanders, A. (1992). An empirical comparison of alternative models of the short-term interest rate. *J. Finance* **47,** 1209–1227.

[6] Conley, T. G., Hansen, L. P., Luttmer, E. G. and Scheinkman, J. A. (1997). Short-term interest rates as subordinated diffusions. *The Review of Financial Studies* **10,** 525–577.

[7] Cox, J., Ingersoll, J. and Ross, S. (1985). A theory of the term structure of interest rates. *Econometrica* **53,** 385–408.

[8] Doukhan, P. (1994). *Mixing. Properties and Examples.* Springer, Berlin.

[9] Feller, W. (1951), Two singular diffusion problems. *Ann. Math.* **54,** 173–182.

[10] Flannery, B. P., Press, W. H., Teukolsky, S. A. and Vetterling, W. T. (1995). *Numerical Recipes in C*, 2nd edn. Cambridge, Cambridge.

[11] Genon-Catalot, V., Jeantheau, T. and Larédo, C. (2000). Stochastic volatility models as hidden Markov models and statistical applications. *Bernoulli* **6,** 1051–1079.

[12] Gyöngy, I. (1998). A note on Euler approximations. *Potential Anal.* **8,** 205–216.

[13] Hansen, N. R. (2003). Geometric ergodicity of dicrete approximations of multivariate diffusions. *Bernoulli* **9,** 725–743.

[14] Hansen, L. P., Scheinkman, J. A. and Touzi, N. (1998). Spectral methods for identifying scalar diffusions. *J. Econometrics* **86,** 1–32.

[15] Higham, D. J. (2000). Mean-square and asymptotic stability of the stochastic Theta method. *SIAM J. Numer. Anal.* **38,** 753–769.

[16] Higham, D. J., Mao, X. and Stuart, A. (2002). Strong convergence of numerical methods for nonlinear stochastic differential equations. *SIAM J. Numer. Anal.* **40,** 1041–1063.

[17] Karatzas, I. and Shreve, S. E. (1991). *Brownian Morion and Stochastic Calculus*, 2nd edn. Springer, Berlin.

[18] Karlin, S. and Taylor, H. M. (1981). *A Second Course in Stochastic Processes*. Academic, New York.

[19] Kloeden, P. E. and Platen, E. (1995). *Numerical Solution of Stochastic Differential Equations*. Springer, Berlin.

[20] Mattingly, J., Stuart, A. and Higham, D. (2002). Ergodicity for SDEs and approximations: locally Lipschitz vector fields and degenerate noise. *Stochastic Process. Appl.* **101,** 185–232.

[21] Petruccelli, J. D. and Woolford, S. W. (1984). A treshold AR(1) model, *J. Appl. Probab.* **21,** 270–286.

[22] Revuz, D. and Yor, M. (1999). *Continuous Martingales and Brownian Motion*. Springer, Berlin.

[23] Rogers, L. C. G. and Williams, D. (1987). *Diffusions, Markov Processes, and Martingales. Volume 2: Itô Calculus*. Wiley, New York.

[24] Talay, D. (2002). Stochastic Hamiltonian dissipative systems with non globally Lipschitz coefficients: exponential convergence to the invariant measure, and discretization by the implicit Euler scheme. *Markov Process. Related Fields* **8,** 163–198.

List of D-CAF's Working Papers
2006 -

1. B.J. Christensen and M. Ørregaard Nielsen (March 2006), *Asymptotic normality of narrow-band least squares in the stationary fractional cointegration model and volatility forecasting.*
2. B.J. Christensen and M. Ørregaard Nielsen (March 2006), *The implied-realized volatility relation with jumps in underlying asset prices*
3. B.J. Christensen and P. Raahauge (March 2006), *Latent utility shocks in a structural empirical asset pricing model*
4. B.J. Christensen and M. Ørregaard Nielsen (March 2006), *The effect of long memory in volatility on stock market fluctuations*
5. T. Busch, B.J. Christensen and M. Ørregaard Nielsen, *Forecasting exchange rate volatility in the presence of jumps* .
6. B.J. Christensen and N.M. Kiefer (March 2006), *Investment in advertising campaigns and search: Identification and inference in marketing and dynamic programming models*
7. T. Busch, B.J. Christensen and M. Ørregaard Nielsen, (March 2006), *The information content of treasury bond options concerning future volatility and price jumps*
8. O.E. Barndorff-Nielsen, P. Reinhard Hansen, A. Lunde and N. Shephard (June 2006), *Designing realised kernels to measure the ex-post variation of equity prices in the presence of noise.*
9. F. Armerin, B. Astrup Jensen, and T. Björk (June 2006), *Term Structure Models with Parallel and Proportional Shifts.*
10. J.M.P. Albin, B. Astrup Jensen, A. Muszta, and M. Richter (June 2006), *On Volatility Induced Stationarity for Stochastic Differential Equations.*